Physical Chemistry Chemical Physics 13: 4507- 4513 (2011)

Towards Biochemical Filter with Sigmoidal Response to pH Changes: Buffered Biocatalytic Signal Transduction

Marcos Pita[#], Vladimir Privman[‡], Mary A. Arugula[‡], Dmitriy Melnikov[‡], Vera Bocharova[‡], Evgeny Katz[‡]*

[#] *Instituto de Catálisis y Petroleoquímica, CSIC, C/Marie Curie 2, 28040 Madrid, Spain*

[‡] *Department of Chemistry and Biomolecular Science, and Department of Physics, Clarkson University, Potsdam, NY 13699, USA*

***** Corresponding author:

E-mail: ekatz@clarkson.edu; Tel.: +1 (315) 268-4421; Fax: +1 (315) 268-6610

Abstract

We realize a biochemical filtering process based on the introduction of a small quantity of a buffer in a biocatalytic signal-transduction logic system based on the function of an enzyme, esterase. The input, ethyl butyrate, is converted into butyric acid—the output signal, which in turn is measured by the drop in the pH value. The developed approach offers a versatile "network element" for increasing the complexity of biochemical information processing systems. Evaluation of an optimal regime for quality filtering is accomplished in the framework of a kinetic rate-equation model.

1. Introduction

As silicon technology is approaching its limits,[1] unconventional approaches to the next generation computing systems are being researched with the hope of offering new functionalities and advances in information processing.[2,3] Molecular (chemical) computing[4-10] has been considered among the approaches to miniaturizing computing elements, as well as novel applications. Biomolecular computing[11-13] can offer an additional advantage of the biochemical specificity of catalytic and recognition processes, ultimately aiming at mimicking and developing systems compatible with the natural information processing mechanisms. Biochemical systems designed for information processing range from various biomolecules, such as proteins,[14,15] DNA,[16] RNA,[17] DNAzymes,[18,19] to whole biological cells operating as computing devices.[20] Enzyme-based biocatalytic systems realizing binary logic gates[11,21-24] and their small networks[25,26] have been recently extensively studied in biomolecular computing.

Despite great expectations for biomolecular computing (biocomputing) systems,[27] the present level of their complexity does not allow any real computing device based on biomolecules. Indeed, only networks performing a few logic operations on a time-scale of minutes have thus far been realized in the lab. However, another application for (bio)molecular information processing has been within reach for the available technology level: extension of capabilities of multi-signal digital biosensors with built-in logic.[28] Such biosensors processing information at the biochemical level are of interest in biomedical applications,[29-32] since biomolecules are capable of operating in a biological environment.[33] Within the general program of the digital biosensor development, several systems of various complexity have recently been designed to analyze pathophysiological conditions corresponding to different injuries.[34-38]

Another promising application of biomolecular logic systems has been for controlling multi-signal responsive materials aiming at chemical actuators with built-in logic.[39] Coupling of the signal-processing enzyme logic systems with switchable "smart" materials can be achieved through redox transformations[40] or pH changes[41-45] driven by the enzyme reactions, offering new "Sense/Act" sensor/actuator functionalities. Specifically, pH changes generated by the

enzyme logic systems, causing polymer materials to switch between different states, have been successfully used to trigger reconfiguration of various nanostructured systems such as membranes,[41] emulsions[42] and nanoparticle assemblies,[43] as well as modified electrodes[46] and bioelectronic devices (biofuel cells).[47]

One of the main challenges for biocomputing has been the design of logic gates that can be combined, with the help of other, enabling non-binary elements, to allow interconnection in fault-tolerant networks with control of noise buildup, for information processing of increasing size and complexity.[48-50] There is ample experimental evidence[48-50] that the level of noise in (bio)chemical computing systems is quite high compared to their electronic counterparts: This includes noise in both the inputs/outputs chemical and the enzyme concentrations which typically vary at least several percent. Thus, the problem of noise amplification and its control becomes an important issue in the design of even small biocomputing networks.[51,52]

One of the possible approaches to noise reduction and control could be the use of filters as network elements converting a convex-shape concentration-response typical of (bio)chemical reactions to a sigmoidal function, thus suppressing noise at the binary **0** and **1** logic points. This could be achieved, for example, by using enzymes with substrates that have self-promoter properties, as biocatalytic elements in logic gates/networks.[53,54] However, this approach requires very specific (e.g., certain allosteric) enzymes and thus cannot be considered as a versatile solution. We have recently reported a general approach to biochemical filter systems based on redox transformations.[55] Since many enzyme logic systems use pH changes as output signals to control pH-responsive materials[41-44] and switchable electrode interfaces,[46,47] an alternative approach devised specifically for pH-change signal filtering would be desirable. The present paper reports the first experimental realization and theoretical modeling of a versatile pH-filter mechanism based on buffering, for enzyme-catalyzed reactions, aiming at noise reduction upon transduction of biochemical signals.

Our system is illustrated in Figure 1. The "logic function" considered is the simplest possible one, that of signal tranmsmission/transduction/conversion: an enzyme-catalyzed reaction converts the concentration of the input chemical into the output signal quantified by

the drop in the pH value. An effect of a small amount of buffer, if added, is to change the system response from convex, as typical for most (bio)chemical processes, to sigmoidal, as desired for filters. Details of our experimental system are presented in Sections 2-3. Careful selection of the system parameters by modeling, is crucial for obtaining a reasonable filtering effect for suppression of noise buildup, as explained in Sections 4-5. Section 6 is devoted to conclusions.

2. Experimental

Esterase from porcine liver (EC 3.1.1.1), ethyl butyrate, 4-(2-hydroxyethyl)-1-piperazineethanesulfonic acid (HEPES buffer), and other inorganic reagents were purchased from Sigma-Aldrich and were used as supplied without any pretreatment or purification. Ultrapure water (18.2 MΩ·cm) from NANOpure Diamond (Barnstead) source was used in all of the experiments.

The enzymatic reactions were carried out in aqueous solutions containing 0 mM, 50 mM and 100 mM of HEPES buffer with ethyl butyrate concentration ranging from 0.1 mM to 100 mM for a fixed amount (4 $U \cdot mL^{-1}$) of esterase. Prior to starting each reaction, the pH of the buffer was adjusted to 7.0 by using 0.1 M NaOH. Once the pH was stable, the reaction was started by adding esterase and monitoring the decrease in the pH value. The experiments were performed under vigorous stirring in a final solution volume of 5 mL. The pH measurements were performed with Mettler Toledo® SevenEasy pH-meter. Using Lab-pH software, the readout of the pH was performed every second. The decrease of pH was measured for the time period of 130 min. Additionally control experiments with butyric acid varied from 0.1 mM to 100 mM, with 0 mM, 50 mM, 100 mM of HEPES buffer were also performed. All experiments were performed at an ambient temperature of 23±2 °C.

3. Biochemical pH-Signal Filter

Our enzymatic biochemical "signal processing" is based on the hydrolysis of ethyl butyrate (substrate, S, serving as the logic input) catalyzed by esterase (enzyme, E) with the butyric acid as the logic output product (P), causing the drop in the pH value. Schematically, we write

$$\mathrm{S} + \mathrm{E} \underset{}{\overset{R}{\leftrightarrows}} \mathrm{C} \overset{r}{\rightarrow} \mathrm{E} + \mathrm{P} \quad (1)$$

where R and r are the forward rates at which the intermediate complex, C, and the final product are formed (the first step can be reversible: we comment on this later). While the output product is the acid molecule,[56,57] we assume that the equilibrium dissociation of butyric acid (A) in solution, with the dissociation constant K_A, is instantaneous: we use the self-explanatory notation

$$\begin{aligned} [\mathrm{P}] &= [\mathrm{A}] + [\mathrm{A}^-] \\ K_A &= [\mathrm{A}^-][\mathrm{H}^+]/[\mathrm{A}] \end{aligned} \quad (2)$$

It is well known[58-60] that the reaction rates R and r for esterase strongly depend on pH of the system: The reaction (1) is fastest at $\mathrm{pH} \sim 9$ and it virtually stops at $\mathrm{pH} \sim 3$. To account for the slowing down of the reaction with decreasing pH, in our parameter range we can assume[58] acidic ionization of the active sites in both the enzyme and intermediate complex, by adding instantaneous dissociation equilibria

$$\begin{aligned} K_E &= [\mathrm{E}][\mathrm{H}^+]/[\mathrm{EH}^+] \\ K_C &= [\mathrm{C}][\mathrm{H}^+]/[\mathrm{CH}^+] \end{aligned} \quad (3)$$

for the ionized enzyme and complex, respectively. We monitor the pH value of the solution as a function of time, t, starting from the reaction's on-set ($t = 0$). This yields kinetic data for the reaction which will be used in the theoretical model to determine the reaction constants and perform system optimization.

We could consider zero initial concentrations of the input substrate and the output product as the logic-**0** values, while the case of the maximum initial substrate concentration and the output product measured at a specific reaction time t — which in practice are set by an application — as corresponding to logic-**1** points. Another option, favored in our present study and used from now on, is to set the logic values for the output at the appropriate pH values. The

"logic range" variables x and y (inset in Figure 1) that vary between 0 and 1, will be defined in the next section. It is important to note that beyond such a "binary" description, in general the plot of the output vs. the initial substrate concentration (viewed as the response curve in terms of the logic-range variable of the type shown in Figure 1) is convex, which is typical for enzymatic reactions; such response amplifies input analog noise.[48-50] Instead, it is desirable to have a sigmoidal response, i.e., the curve should be "flat" around both logic points and with inflection in between. Indeed, such a response curve offers the filtering effect by decreasing analog noise at each logic point.[55]

While such a sigmoidal response is observed in nature,[50,61-63] it is generally not easy to realize in biochemical reactions.[52,55] In this work, we attempt to artificially create sigmoidal response of the pH variation in an enzyme-catalyzed reaction: We introduce, see Figure 1, a buffer (B), here HEPES. The latter is a weak acid with the dissociation constant satisfying $K_{\mathrm{HEPES}} \ll K_A$,

$$K_{\mathrm{HEPES}} = [\mathrm{B}^-][\mathrm{H}^+]/[\mathrm{B}] \quad (4)$$

Usually HEPES is used in large enough quantities as a buffer[64,65] for biological systems to maintain constant pH during experiments. In our case, however, the largest amounts of HEPES are comparable to the maximum initial substrate concentration. This means that in the beginning of reaction or for small substrate concentrations, i.e., close to the logic-**0**, HEPES will operate as a buffer and keep the pH of the solution at a constant, initially titrated level. When more acid is produced in the enzymatic reaction (1), the buffering capacity of HEPES will eventually be overwhelmed, and the pH will rapidly decrease and stay constant at the level determined by K_A and the final amount of the produced butyric acid. As a result an inflection region appears on the curve of pH vs. the initial substrate concentration which thus becomes sigmoidal. Note that the presence of a small quantity of the buffer significantly modifies the system's response only near logic-**0** of the input, whereas the response curve near logic-**1** is typically sufficiently "flat" anyway, as described earlier.[50,55]

However, additional challenges arise in this approach. Ideally, we would like to have such an amount of HEPES that the "flat" low-noise regions extent far around both logic points.[52,55] However, if there is too little HEPES, then it will be quickly overwhelmed even by

small amounts of butyric acid so that the small-slope region at logic-**0** will be very narrow. On the other hand, when the amount of HEPES is large, it will act as a buffer throughout the entire range of input concentrations so that the pH at logic-**1** will be close to that at logic-**0**, and it may become difficult to distinguish between the outputs at those two logic points. Furthermore, too much HEPES can increase the slope at logic-**1**, because the reaction will be slowed down and away from saturation. Thus, the problem of establishing the optimal concentration of the buffer for adequate suppression of the analog noise over the broad range of the logic input concentrations around each logic point requires numerical optimization based on the initial data fits. This is illustrated in Section 5.

Figure 2 exemplifies the filtering effect by showing sets of data taken for increasing amounts of HEPES. While the onset of the sigmoidal behavior is clearly seen, the plots also illustrate that the data are noisy, as typical for such enzymatic systems. Figure 3 shows the pH dependence on the reaction time t and initial substrate concentration, for 100 mM of HEPES. For later times ($t > 20$ min) and large enough ethyl butyrate concentrations (over approximately 20 mM), the pH decrease slows down, resulting in a flat region, which illustrates the saturation mentioned earlier, typical of enzymatic processes. Similar trends in the pH dependence were observed also for other studied concentrations of HEPES. We note that the experimental data here are also noisy, which underscores the importance of parameter selection for the filtering effect in such a way that good separation is maintained between the "logic" reference values.

4. Kinetic Equations and Noise Analysis

In order to analyze our data, exemplified in Figures 2 and 3, we use a kinetic rate-equation description of the processes involved. We already noted the complexity of the process steps involved. For a realistic description, we therefore have to limit the number of fitted rate constants utilized. This has been a standard practice in such applications because we seek a semi-quantative overall description of the response surface of the process, with the detailed behavior relevant for signal handling only near the logic-point values. Thus, we use a simplified

kinetic description of reaction (1) assuming no reversibility in the formation of the intermediate complex. Indeed, the available kinetic data[60] for this type of reaction suggest that, in our regime of the parameters, for most of our pH range (except perhaps in the far saturation regime), for the reactant concentrations used, the rate of the reverse reaction will be negligibly small. Furthermore, we use a description whereby the rate equations for hydrolysis process (1), are written in terms of the total (active and acidified) enzyme and complex concentrations, whereas the reduction in the process rates due to the acidification equilibria is lumped in the effective rate parameters $R'(t)$ and $r'(t)$, which replace R and r in (1). We have

$$\begin{aligned} \frac{d[\mathrm{S}]}{dt} &= -R'(t)[\mathrm{S}]\{E_0 - [\mathrm{C}]\} \\ \frac{d[\mathrm{C}]}{dt} &= R'(t)[\mathrm{S}]\{E_0 - [\mathrm{C}]\} - r'(t)[\mathrm{C}] \\ \frac{d[\mathrm{P}]}{dt} &= r'(t)[\mathrm{C}] \end{aligned} \quad (5)$$

where E_0 is the total initial amount of the enzyme, and, as mentioned, we ignore the acidification shown in (3), instead using the effective rate parameters

$$\begin{aligned} R'(t) &= \frac{K_E}{[\mathrm{H}^+](t) + K_E} R \\ r'(t) &= \frac{K_C}{[\mathrm{H}^+](t) + K_C} r \end{aligned} \quad (6)$$

The concentration $[\mathrm{H}^+](t)$ in (6), which yields the pH value, is determined from the charge balance equation. Since the enzyme and complex concentrations are very small compared to other chemicals, we can neglect their contributions. The resulting equation is

$$[\mathrm{H}^+](t) = [\mathrm{H}^+]_0 + \frac{K_A}{K_A + [\mathrm{H}^+](t)}[\mathrm{P}](t) + \frac{K_{\mathrm{HEPES}}}{K_{\mathrm{HEPES}} + [\mathrm{H}^+](t)}[\mathrm{HEPES}] - [\mathrm{B}^-]_0 \quad (7)$$

where $[\mathrm{H}^+]_0 = 10^{-7}$ M is the concentration corresponding to the initial titration of the system to $\mathrm{pH}_0 = 7$; $[\mathrm{B}^-]_0$ denotes the initial concentration of the HEPES anions after its instantaneous dissociation equilibration (at $\mathrm{pH}_0 = 7$), whereas the total amount of HEPES introduced has been, as a concentration, denoted by [HEPES] already in the captions Figures 1–3. As a result of a numerical solution of the various coupled equations introduced, we can obtain the dependence of the pH(t) on the reaction time.

As alluded to earlier, there are several sources of noise[11,52,55] in biochemical information processing at the level of network elements, as well as at the level of the network as a whole. The buildup of noise must be avoided to allow scalability and fault tolerance. The former, single-element (gate) noise results, for instance, from the inaccuracy of the logic function itself, as seen in Figures 2 and 3, and reflects fluctuations in the chemical concentrations and other experimental conditions and parameters. Our aim is to design network elements that will minimize such analog noise *amplification* as the signal is processed. Other types of noise, specifically, digital noise, are handled at the network-design level, not addressed here. Filtering is the primary tool for avoiding amplification of analog noise. This property of a filter can be quantified as follows.

We define dimensionless logic-range input (x) and output (y) variables, encountered earlier (see the inset in Figure 1):

$$x = \frac{[\mathrm{S}](t=0)}{[\mathrm{S}]_{\max}(t=0)} \quad (8)$$

$$y = \frac{\mathrm{pH}_0 - \mathrm{pH}(t)}{\mathrm{pH}_0 - \mathrm{pH}_{[\mathrm{s}]_{\max}}(t)} = F(x) \quad (9)$$

where $[\mathrm{S}]_{\max}(t=0)$ is the maximum initial concentration (here 100 mM) of the input substrate in our experiments, selected as logic-**1**; pH_0 was defined earlier (=7); and $\mathrm{pH}_{[\mathrm{s}]_{\max}}(t)$ is the output value at the reference time t for the logic-**1** input, i.e., for $[\mathrm{S}]_{\max}(t=0)$, which thus defines the logic-**1** of the output. Thus, the gate-response function $y = F(x)$, for our trivial, "identity" gate connects the logic points at $(x, y) = (0,0)$ and $(1,1)$.; see Figure 1 inset.

The response function (9) can be calculated from the presented solution once four adjustable parameters, R, r, K_E, K_C are first determined from a least-squares fit of the experimentally measured pH data, as reported in the next section. Other quantities and parameters are known or were taken from the literature; the latter were the tabulated values for $\mathrm{p}K_A = 4.83$ and $\mathrm{p}K_{\mathrm{HEPES}} = 7.55$, which were validated by performing control experiments in which butyric acid and HEPES were mixed directly.

With the response function $F(x)$ calculated, we perform numerical analysis[48,50] of our logic filter to gauge its noise amplification/suppression properties in the vicinity of the two logic points, **0** and **1**. We define the noise amplification factor as the ratio of the maximum of the two output noise distribution spreads, σ_i^{out} (computed for each logic point, $i = 0, 1$) and the input noise spread, $\max(\sigma_i^{out}/\sigma^{in})$. Here the spread of the output distribution is defined as the root-mean-square width, for instance,

$$\sigma_i^{out} = [\langle y^2 \rangle_i - \langle y \rangle_i^2]^{1/2} \quad (10)$$

with the averages $\langle \cdots \rangle$ at each logic point are computed with respect to the input noise distribution function which is assumed to be Gaussian with the same variance, σ^{in}, at both $i = 0, 1$. (Actually, half-Gaussian for a logic point with only positive signal values physically possible, such as our logic-**0** input, [S] = 0.) This ratio allows us to determine how large are the deviations in the output signal as compared to the assumed spread in the input signal. For a good filter, $\max(\sigma_i^{out}/\sigma^{in})$ should be less than 1 (means, noise suppression) for typical input signal spread values in biochemical systems, which have σ^{in} at least a couple of percent on the scale of the logic-interval range of 1.

5. Results

Experimentally measured dependence of the pH on the reaction time *t* and initial ethyl butyrate (substrate) concentration is illustrated in Figures 2 and 3. Our data fitting included all the recorded time-dependent data, for several HEPES concentrations and varying input substrate values, similar to Figure 3. This yielded the estimates: $R = 60.0 \pm 0.2\ (\text{mM} \cdot \text{s})^{-1}$, $r = 26.9 \pm 0.7\ \text{s}^{-1}$, $K_E = 0.00680 \pm 0.00003$ mM, and $K_C = 0.020 \pm 0.006$ mM. The quality of the least-squares fits was quite good. Note that $K_C \gg K_E$, similar to the results found earlier with methyl-*n*-butyrate as the substrate for esterase.[58]

The onset of the sigmoidal profile in the response curves can be seen in Figure 2, and is also clearly present in the data shown in Figure 3. Specifically, Figure 2 shows how pH of the system depends on the substrate concentration at a fixed reaction time, 120 min experimental section says 130 min, for increasing amounts of HEPES: 0, 50, 100 mM. As expected, with

larger concentrations of HEPES the response curves around logic-**0** point become more "flat" whereas the slopes at logic-**1** slightly increase. This is also seen in the inset in Figure 1, where the same data and fitted curves are shown in terms of the logic-range variables, *y* vs. *x*. A tradeoff involved in getting the filtering effect is the trend, clearly visible in Figure 2, of decreasing the difference between the pH values at the two logic points, $\Delta\mathrm{pH}_{01} = \mathrm{pH}_0 - \mathrm{pH}_1$. This occurs because the pH-drop signal buildup is delayed by the filtering effect. Without HEPES we have $\Delta\mathrm{pH}_{01}$~4.1, but this difference drops to ~2.7 for [HEPES] = 100 mM. This property may make it more difficult to distinguish between the outputs (pH values) at logic-**0** and **1** in real life applications, due to another source of noise, obvious in Figure 2 and 3: the intrinsic noise in the logic-element functioning itself (whereas filtering is aimed at reducing noise *amplification* from input to output).

The numerically evaluated dependence of the maximum (over the two logic-point values) noise amplification factor, $\max(\sigma_i^{out}/\sigma^{in})$, vs. reaction time t and HEPES concentration is shown in Figure 4, assuming a rather large input noise spread, $\sigma^{in} = 0.3$ (30%). The dots correspond to the experimental conditions at which data shown in Figure 2 were obtained. With increasing time and HEPES concentration, $\max(\sigma_i^{out}/\sigma^{in})$ decreases until it reaches its minimum, for at $t \sim 50\text{–}150$ min, [HEPES] ~ 300 mM (this region is marked in the figure). Note that in this region we have $\max(\sigma_i^{out}/\sigma^{in}) \sim 0.7 < 1$, which does indicate noise suppression. However, this value is still not vanishingly small because at $\sigma^{in} = 0.3$ there is a noticeable contribution to the output signal from the parts of the response curve with large slope (close to the inflection). For smaller noise spread (than the assumed 30%) the filtering effect will actually be somewhat better, but the overall results and trends are qualitatively similar.

The region of the optimal noise suppression marked in Figure 4, is particularly interesting for potential applications because in addition to a small noise amplification factor (~ 0.7), the pH variation between the two logic points is not much reduced: $\Delta\mathrm{pH}_{01}$ is ~ 2 or larger; see Figure 5. We point out that, in Figure 4 there is another range of the reaction times and HEPES concentrations for which $\max(\sigma_i^{out}/\sigma^{in}) < 1$. It is located at $t \sim 50$ min and [HEPES] > 300 mM. However, as can be seen from Figure 5, in this region $\Delta\mathrm{pH}_{01}$ is

somewhat smaller than ~ 1, which makes this range of parameters less favorable for filter operation.

Around logic-**0** point, when pH deviates only a little from its initial titration value, pH_0, we can expand (7) in Taylor series and obtain analytical expression for the slope of the response curve. This yields additional information on which of the system parameters influence noise characteristics the most. Since $[\mathrm{H}^+]_0 \ll [\mathrm{B}]_0$, we get for the response curve slope

$$\left.\frac{d\mathrm{pH}}{d[\mathrm{S}]}\right|_0 \approx [\mathrm{HEPES}]^{-1}\left(\sqrt{\frac{K_{\mathrm{HEPES}}}{[\mathrm{H}^+]_0}}+\sqrt{\frac{[\mathrm{H}^+]_0}{K_{\mathrm{HEPES}}}}\right)^2 \qquad (11)$$

From this expression we see not only that the increasing buffer concentration leads to a smaller slope and consequently, stronger noise suppression, as expected, but also that the initial pH and the buffer dissociation constant also affect filter performance. In particular, in order to keep analog noise in check, one cannot indiscriminately vary pH_0. Indeed, for different pH another buffer would be preferable, with its dissociation constant compatible with the new pH value. Then the optimal analog noise suppression at logic-**0** will be possible. Note that this condition is relatively well met by our system: $\mathrm{pH}_0 = 7 \sim \mathrm{p}K_{\mathrm{HEPES}} = 7.55$.

6. Conclusion

In this work we experimentally demonstrated a biochemical logic filter with artificially induced sigmoid pH-drop response. We used esterase-catalyzed hydrolysis of ethyl butyrate as the substrate. By performing this reaction in the HEPES buffer supplied in limited amounts, we were able to suppress the change in the pH at small initial concentrations of the substrate. As a result, the response curve of the filter (dependence of the pH on substrate concentration) changes to the sigmoid one for which analog noise can in principle be suppressed around both logic points provided that we have the correct amount of HEPES in our system and properly select other system parameters as discussed in Section 4.

We performed kinetic modeling of the system and determined the optimal required amount of HEPES and reaction times at which maximum noise suppression occurs. For this, we first numerically fitted the experimental response surfaces to the solution of the system of kinetic and charge balance equations, thus fixing the unknown reaction parameters. With these quantities known, we were able to study general noise properties of this system as functions of the HEPES concentration and reaction time. We found that the optimal amount of HEPES at which maximum suppression of noise occurs is ~ 300 mM, with reaction times $\sim 50-150$ min. We also found that in general, optimum performance of the filter is possible only provided one works with systems such that the initial pH is close to the (minus decimal logarithm of the) dissociation constant of the selected weak-acid buffer. The method as described, is easy to realize in practice and shows promise for use in information processing networks, because no cross-reactions are introduced: the buffer acid is typically not a part of the (bio)chemical processes in the system.

Acknowledgements

The authors thank Dr. J. Halámek for helpful scientific input and collaboration. The work in Spain (M.P.) was funded by Ramón y Cajal program, MICINN. We acknowledge research funding by the US-NSF, under grant CCF-1015983.

References

1 *The International Technology Roadmap for Semiconductors* (ITRS), 2009 Edition, maintained online at http://www.itrs.net by the sponsoring organizations: the European Semiconductor Industry Association (ESIA), the Japan Electronics and Information Technology Industries Association (JEITA), the Korean Semiconductor Industry Association (KSIA), the Taiwan Semiconductor Industry Association (TSIA), and the United States Semiconductor Industry Association (SIA).

2 *Unconventional Computation. Lecture Notes in Computer Science*, C. S. Calude, J. F. Costa, N. Dershowitz, E. Freire and G. Rozenberg (Eds.), Vol. 5715, Springer, Berlin, 2009.

3 *Unconventional Computing*, A. Adamatzky, B. De Lacy Costello, L. Bull, S. Stepney and C. Teuscher (Eds.), Luniver Press, UK, 2007.

4 A. P. de Silva, S. Uchiyama, T. P. Vance and B. Wannalerse, *Coord. Chem. Rev.*, 2007, **251**, 1623–1632.

5 A. P. de Silva and S. Uchiyama, *Nature Nanotechnology*, 2007, **2**, 399–410.

6 K. Szacilowski, *Chem. Rev.*, 2008, **108**, 3481–3548.

7 A. Credi, *Angew. Chem. Int. Ed.*, 2007, **46**, 5472–5475.

8 U. Pischel, *Angew. Chem. Int. Ed.*, 2007, **46**, 4026–4040.

9 U. Pischel, *Austral. J. Chem.*, 2010, **63**, 148–164.

10 J. Andreasson and U. Pischel, *Chem. Soc. Rev.*, 2010, **39**, 174–188.

11 E. Katz and V. Privman, *Chem. Soc. Rev.*, 2010, **39**, 1835–1857.

12 A. Saghatelian, N. H. Volcker, K. M. Guckian, V. S. Y. Lin and M. R. Ghadiri, *J. Am. Chem. Soc.*, 2003, **125**, 346–347.

13 G. Ashkenasy and M. R. Ghadiri, *J. Am. Chem. Soc.*, 2004, **126**, 11140–11141.

14 S. Sivan, S. Tuchman and N. Lotan, *Biosystems*, 2003, **70**, 21–33.

15 R. Unger and J. Moult, *Proteins*, 2006, **63**, 53–64.

16 M. N. Stojanovic, D. Stefanovic, T. LaBean and H. Yan, in: *Bioelectronics: From Theory to Applications*, I. Willner and E. Katz (Eds.), Wiley-VCH, Weinheim, 2005, pp. 427–455.

17 M. N. Win and C. D. Smolke, *Science*, 2008, **322**, 456–460.

18 S. Bi, Y. M. Yan, S. Y. Hao and S. S. Zhang, *Angew.Chem. Int. Ed.*, 2010, **49**, 4438–4442.

19 T. Li, E. K. Wang and S. J. Dong, *J. Am. Chem. Soc.*, 2009, **131**, 15082–15083.

20 M. L. Simpson, G. S. Sayler, J. T, Fleming and B. Applegate, *Trends Biotechnol.*, 2001, **19**, 317–323.

21 R. Baron, O. Lioubashevski, E. Katz, T. Niazov and I. Willner, *J. Phys. Chem. A*, 2006, **110**, 8548–8553.

22 R. Baron, O. Lioubashevski, E. Katz, T. Niazov and I. Willner, *Angew. Chem. Int. Ed.*, 2006, **45**, 1572–1576.

23 G. Strack, M. Pita, M. Ornatska and E. Katz, *ChemBioChem*, 2008, **9**, 1260–1266.

24 J. Zhou, M. A. Arugula, J. Halámek, M. Pita and E. Katz, *J. Phys. Chem. B*, 2009, **113**, 16065-16070.

25 T. Niazov, R. Baron, E. Katz, O. Lioubashevski and I. Willner, *Proc. Natl. Acad. USA.*, 2006, **103**, 17160-17163.

26 G. Strack, M. Ornatska, M. Pita and E. Katz, *J. Am. Chem. Soc.*, 2008, **130**, 4234-4235.

27 P. Fu, *Biotechnol. J.*, 2007, **2**, 91–101.

28 J. Wang and E. Katz, *Anal. Bioanal. Chem.*, 2010, **398**, 1591–1603.

29 R. Adar, Y. Benenson, G. Linshiz, A. Rosner, N. Tishby and E. Shapiro, *Proc. Natl. Acad. USA.*, 2004, **101**, 9960–9965.

30 F. C. Simmel, *Nanomedicine*, 2007, **2**, 817–830.

31 E. E. May, P. L. Dolan, P. S. Crozier, S. Brozik and M. Manginell, *IEEE Sens. J.*, 2008, **8**, 1011–1019.

32 G. von Maltzahn, T. J. Harris, J.-H. Park, D.-H. Min, A. J. Schmidt, M. J. Sailor and S. N. Bhatia, *J. Am. Chem. Soc.*, 2007, **129**, 6064–6065.

33 M. Kahan, B. Gil, R. Adar and E. Shapiro, *Phisica D*, 2008, **237**, 1165–1172.

34 M. Pita, J. Zhou, K. M. Manesh, J. Halámek, E. Katz and J. Wang, *Sens. Actuat. B*, 2009, **139**, 631–636.

35 K. M. Manesh, J. Halámek, M. Pita, J. Zhou, T. K. Tam, P. Santhosh, M.-C. Chuang, J. R. Windmiller, D. Abidin, E. Katz and J. Wang, *Biosens. Bioelectron.*, 2009, **24**, 3569–3574.

36 J. R. Windmiller, G. Strack, M.-C. Chuan, J. Halámek, P. Santhosh, V. Bocharova, J. Zhou, E. Katz and J. Wang, *Sens. Actuat. B*, 2010, **150**, 285–290.

37 J. Halámek, J. R. Windmiller, J. Zhou, M.-C. Chuang, P. Santhosh, G. Strack, M. A. Arugula, S. Chinnapareddy, V. Bocharova, J. Wang and E. Katz, *Analyst*, 2010, **135**, 2249–2259.

38 J. Halámek, V. Bocharova, S. Chinnapareddy, J. R. Windmiller, G. Strack, M.-C. Chuang, J. Zhou, P. Santhosh, G. V. Ramirez, M. A. Arugula, J. Wang and E. Katz, *Mol. BioSyst.*, 2010, in press (DOI: 10.1039/c0mb00153h.).

39 M. Pita, S. Minko and E. Katz, *Journal of Materials Science: Materials in Medicine*, 2009, **20**, 457–462.

40 G. Strack, V. Bocharova, M. A. Arugula, M. Pita, J. Halámek and E. Katz, *J. Phys. Chem. Lett.*, 2010, **1**, 839–843.

41 I. Tokarev, V. Gopishetty, J. Zhou, M. Pita, M. Motornov, E. Katz and S. Minko, *ACS Appl. Mater. Interfaces*, 2009, **1**, 532–536.

42 M. Motornov, J. Zhou, M. Pita, I. Tokarev, V. Gopishetty, E. Katz and S. Minko, *Small*, 2009, **5**, 817–820.

43 M. Motornov, J. Zhou, M. Pita, V. Gopishetty, I. Tokarev, E. Katz and S. Minko, *Nano Lett.*, 2008, **8**, 2993–2997.

44 V. Bychkova, A. Shvarev, J. Zhou, M. Pita and E. Katz, *Chem. Commun.*, 2010, **46**, 94-96.

45 V. Bocharova, T. K. Tam, J. Halámek, M. Pita and E. Katz, *Chem. Commun.*, 2010, **46**, 2088–2090.

46 M. Privman, T. K. Tam, M. Pita and E. Katz, *J. Am. Chem. Soc.*, 2009, **131**, 1314–1321.

47 E. Katz and M. Pita, *Chem. Eur. J.*, 2009, **15**, 12554–12564.

48 D. Melnikov, G. Strack, M. Pita, V. Privman and E. Katz, *J. Phys. Chem. B*, 2009, **113**, 10472–10479.

49 V. Privman, M. A. Arugula, J. Halámek, M. Pita and E. Katz, *J. Phys. Chem. B*, 2009, **113**, 5301–5310.

50 V. Privman, G. Strack, D. Solenov, M. Pita and E. Katz, *J. Phys. Chem. B*, 2008, **112**, 11777–11784.

51 M. A. Arugula, J. Halámek, E. Katz, D. Melnikov, M. Pita, V. Privman and G. Strack, *Second International Conference on Advances in Circuits, Electronics and Micro-Electronics*, Proceedings, IEEE Comp. Soc. Publ. (Los Alamitos, California) 2009, 1–7.

52 V. Privman, *Israel J. Chem.*, 2011, in press (e-print available on-line at http://arxiv.org/abs/1010.1853).

53 V. Privman, V. Pedrosa, D. Melnikov, M. Pita, A. Simonian and E. Katz, *Biosens. Bioelectron.*, 2009, **25**, 695–701.

54 V. Pedrosa, D. Melnikov, M. Pita, J. Halámek, V. Privman, A. Simonian and E. Katz, *International Journal of Unconventional Computing* 2011, in press (e-print available on-line at http://arxiv.org/abs/0912.4710).

55 V. Privman, J. Halámek, M. A. Arugula, D. Melnikov, V. Bocharova and E. Katz, *J. Phys. Chem. B*, 2010, **114**, 14103–14109.

56 R. B. Silverman, *The Organic Chemistry of Enzyme-Catalyzed Reactions, Revised Edition*, Academic Press, San Diego, 2000, Chapter II, page 60.

57 F. A. Carey and R. J. Sundberg, *Advanced Organic Chemistry, Part A: Structure and Mechanisms*, Springer, New York, 2007, Chapter 2, page 217.

58 N. C. Craig and G. B. Kristiakowsky, *J. Am. Chem. Soc.*, 1958, **80**, 1574–1579.

59 F. Bergmann and S. Rimon, *Biochem. J.*, 1958, **70**, 339–344.

60 A. J. Adler and G. B. Kristiakowsky, *J. Am. Chem. Soc.*, 1962, **84**, 695–703.

61 N. E. Buchler, U. Gerland and T. Hwa, *Proc. Natl. Acad. Sci. USA*, 2005, **102**, 9559–9564.

62 Y. Setty, A. E. Mayo, M. G. Surette and U. Alon, *Proc. Natl. Acad. Sci. USA*, 2003, **100**, 7702–7707.

63 U. Alon, *An Introduction to Systems Biology. Design Principles of Biological Circuits*, Chapman & Hall/CRC Press, Boca Raton, Florida, 2007.

64. N. E. Good, G. D. Winget, W. Winter, T. N. Connolly, S. Izawa, and R. M. M. Singh, *Biochemistry*, 1966, **5**, 467–477.

65. W. J. Ferguson, K. I. Braunschweiger, W. R. Braunschweiger, J. R. Smith, J. J. McCormick, C. C. Wasmann, N. P. Jarvis, D. H. Bell, and N. E. Good, *Anal. Biochem.*, 1980, **104**, 300–310.

Figure Captions

Figure 1. Schematic presentation of the buffering-based pH-signal "logic filter." The reaction biocatalyzed by an enzyme, here esterase, results in the hydrolysis of ethyl butyrate (the logic *Input*) to yield butyric acid which releases H^+ ions upon dissociation. A limited quantity of a buffer, here HEPES, if introduced, consumes most of the biocatalytically produced H^+ ions when the input is applied at a low concentration. The pH change (the logic *Output*, measured by the pH drop, as indicated by an arrow) sets in when the biocatalytically produced H^+ ions overwhelm the buffer. The biocatalytic process and buffering combined, yield a sigmoidal dependence of the pH change as a function of the input concentration. The inset illustrates the onset of the sigmoidal response in our experimental system. The solid curves show the output, *y*, vs. the input, *x*, properly redefined/rescaled to vary in the "binary-logic ranges" from 0 to 1, as explained in the text. Experimental data were fitted by using rate equations appropriate for the processes involved, and the results are shown, here for the reaction time 120 min experimental section says 130 min, for increasing buffer (HEPES) concentrations. The top (red) curve corresponds to [HEPES] = 0; middle (blue): [HEPES] = 50 mM, bottom (green): [HEPES] = 100 mM. The dashed black curve does not correspond to experimental data but rather illustrates a desirable, "ideal" filter response with small slopes at both binary logic points **0** and **1**, and with a steep, symmetrically positioned inflection region in the middle.

Figure 2. Measured pH values at the reaction time $t = 120$ min i120 **1 120 or 130**? ?, is it 120 or 130? shown vs. the initial substrate concentration, for different amounts of HEPES. Red (bottom) symbols/curve correspond to [HEPES] = 0, blue (middle): [HEPES] =50 mM, green (top): [HEPES] = 100 mM. The circular symbols are the actual pH values, whereas the solid curves are the theoretical model fits. (These curves were shown in the inset in Figure 1, rescaled in terms of the logic-range variables).

Figure 3. Top: Experimental dependence of pH on the initial substrate concentration (ethyl butyrate) and reaction time, for [HEPES] = 100 mM. Bottom: Numerically computed dependence for this system, based on the kinetic model.

Figure 4. Color-coded contour plots of the noise amplification factor $\max(\sigma_i^{out}/\sigma^{in})$ as a function of the concentration [HEPES] and reaction time *t*. The dots mark the conditions corresponding to the curves in Figure 2. The broken-line ellipse encircles the optimal-parameter region of filter operation, i.e., times and HEPES concentrations for which the strongest suppression of analog noise is possible.

Figure 5. Color-coded contour plots of ΔpH_{01}. All axes, notation, and markings are the same as in Figure 4.

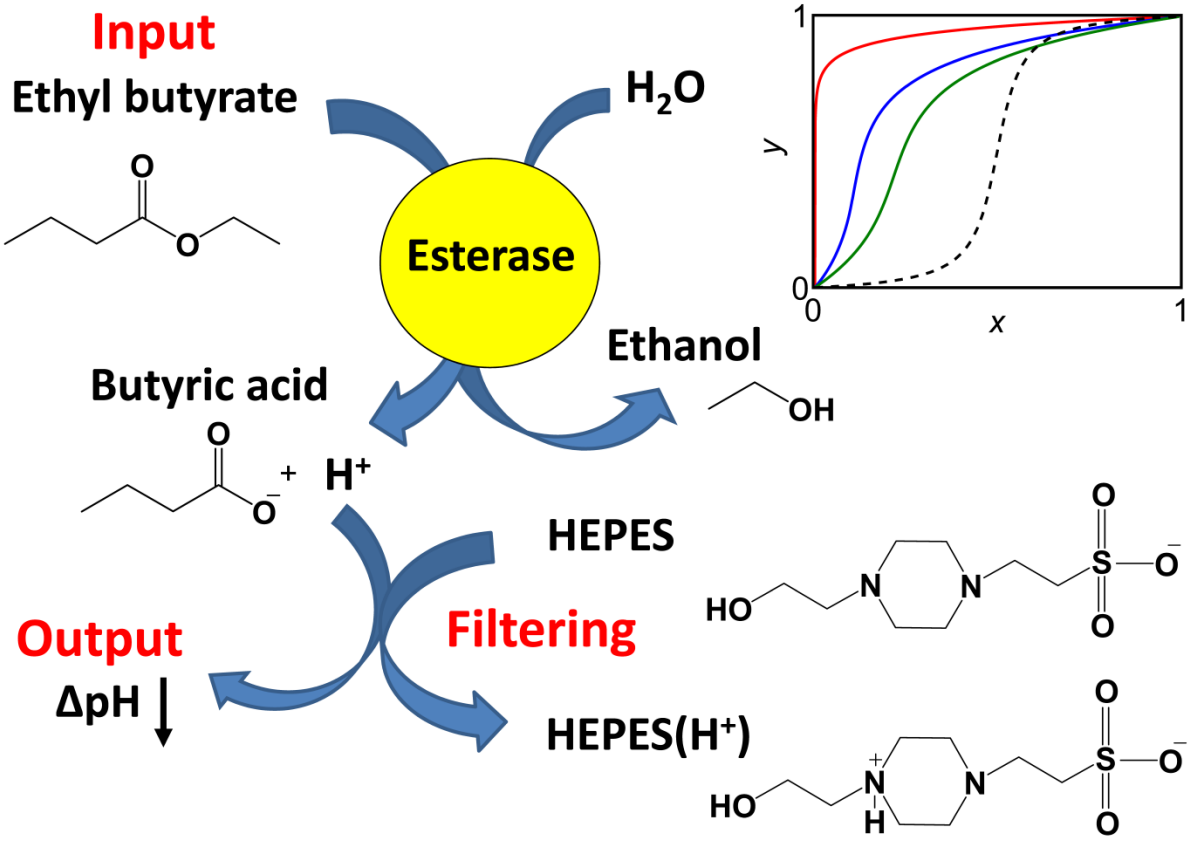

Pita et al.: Figure 1

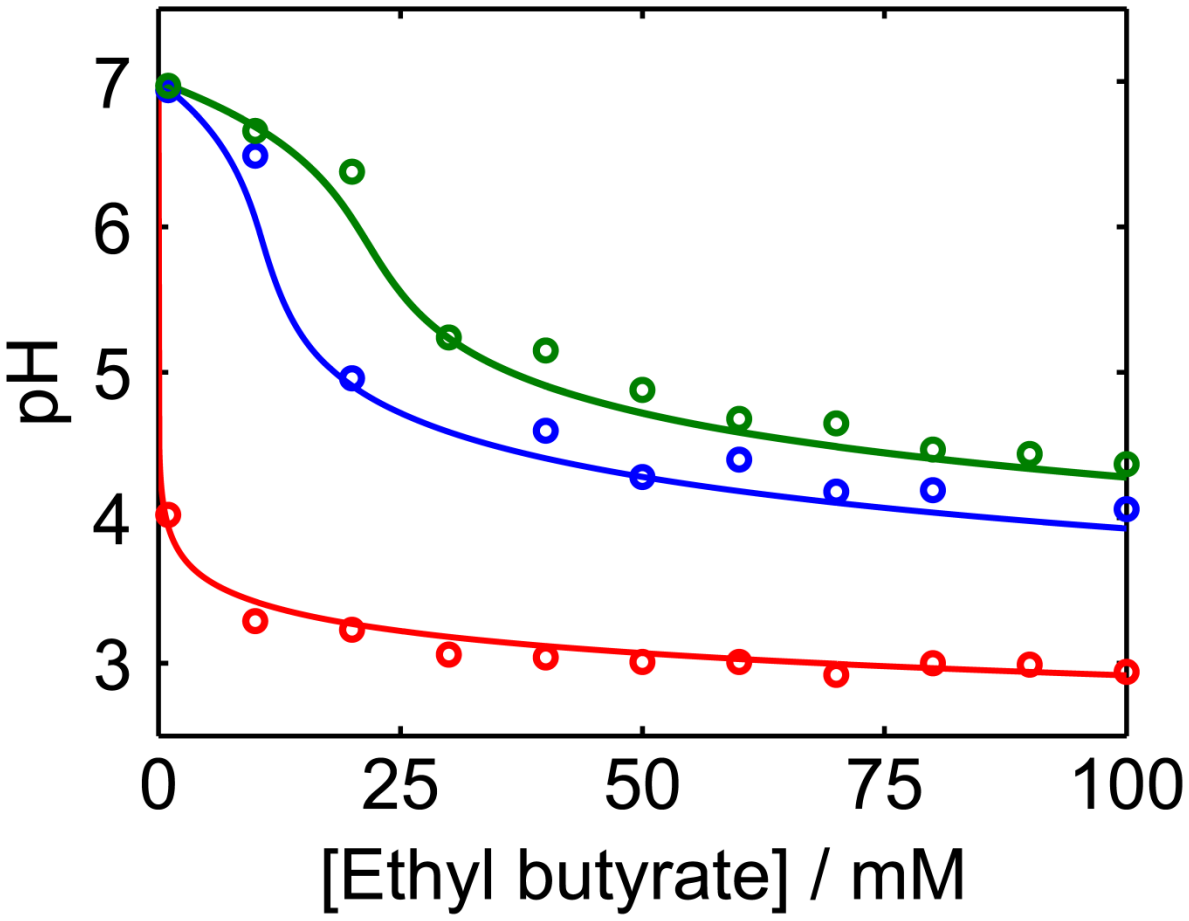

Pita et al.: Figure 2

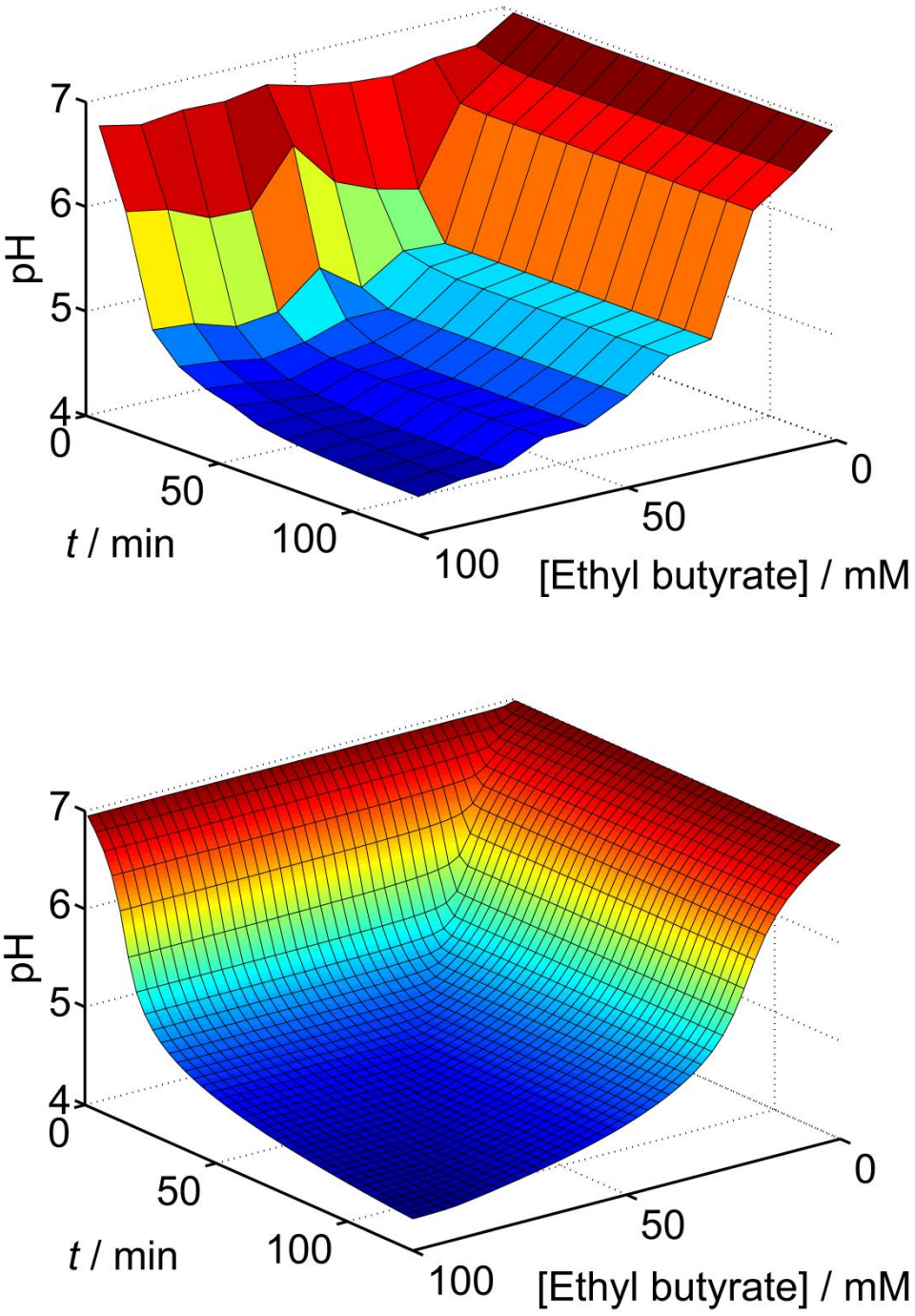

Pita et al.: Figure 3

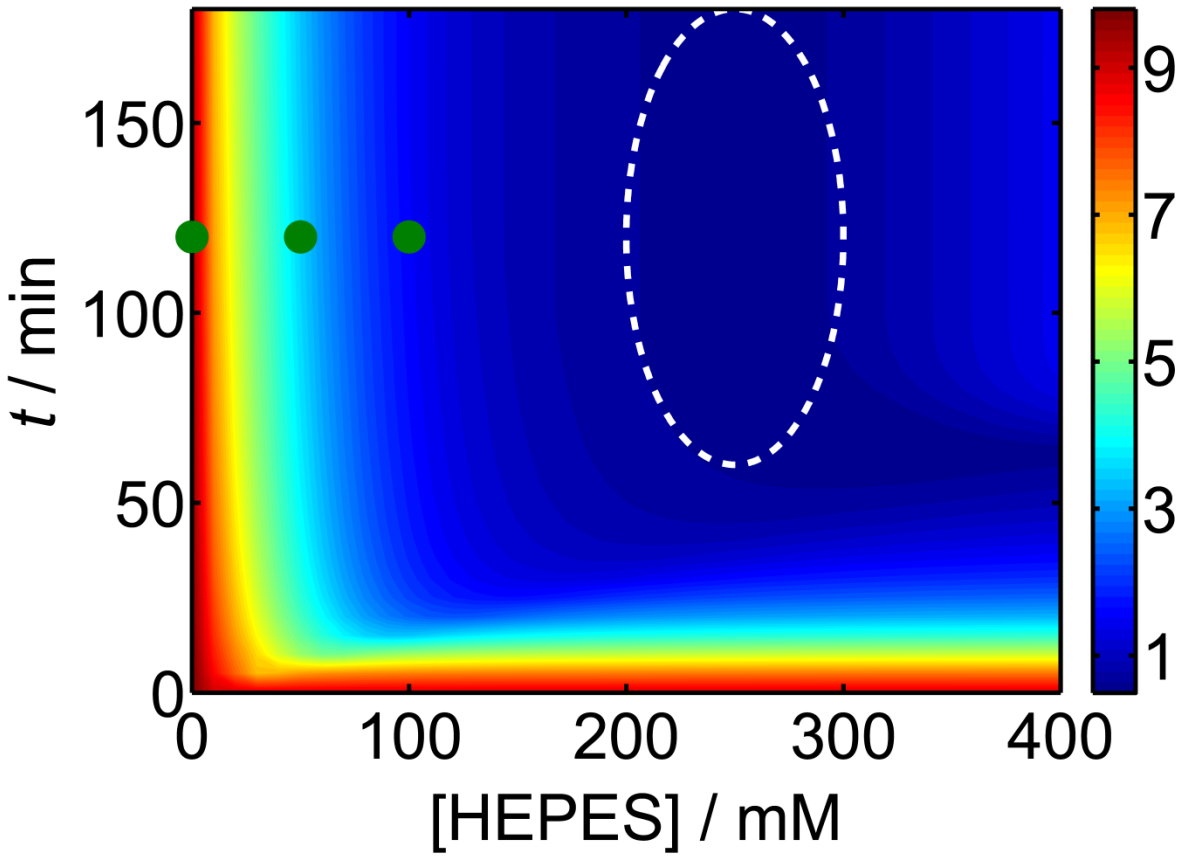

Pita et al.: Figure 4

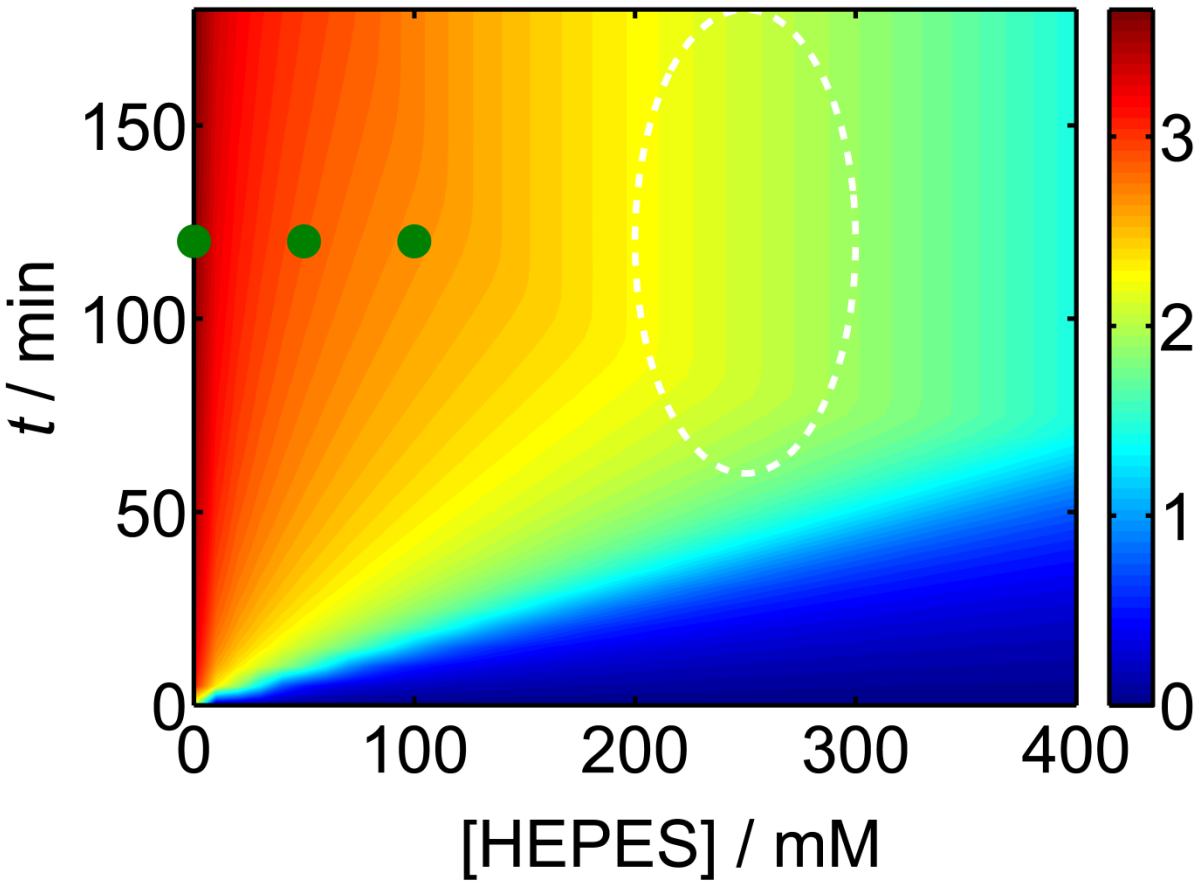

Pita et al.: Figure 5